ISSN: 2277-9655
Impact Factor: 4.116

IJESRT

INTERNATIONAL JOURNAL OF ENGINEERING SCIENCES & RESEARCH TECHNOLOGY

STRUCTURAL AND TRANSPORT PROPERTIES OF TE DOPED LAMNO3

Zafaran Abdul Fattah
Physics Department, Faculty of Education – Zingbar – Aden University

DOI: 10.5281/zenodo.61478

ABSTRACT

The main aim of this project is to study the structural and transport properties of La1-xTexMnO3at (x=0.1 and 0.15). The brief discussion on the progress of this project is given that the samples were characterized using x-ray diffraction (XRD) technique. This gives the information of the crystal symmetry, structure and lattice parameters, which varies with the Te concentration. Further, the electrical resistivity data, which confirm the effect of carrier doping in the system, was analyzed. The resistivity data was also fitted in the Mott's variable range hopping (VRH) model in the high temperature regime, as a result of those processes the unit cell volume of the sample decrease with the increase in Te concentration, the crystallite size increases with the increase in Te concentration. On decreasing the temperature thisLa1-xTexMnO3 first undergoes insulating to metallic phase transition at transition temperatures Tp=203 and 209oK respectively, then resuming the semiconducting behavior, the samples are found to be in single phase. The charge ordering transition temperature of La1-xTexMnO3 is enhanced within Te concentration (Tco=125 to 135oK), the magneto resistance as a function of temperature is also studied in the presence of magnetic of the magnetic fields.

KEYWORDS: Provskite material, La1-xTexMnO3, Mott's VRH model, x-ray diffraction, temperature dependence of magneto–resistance (MR), optical, magnetic, thermoelectric powerand dc conduction measurement.

INTRODUCTION

Transition metal oxides (TMO's) constitute one of the most fascinating classes of inorganic solid exhibiting structural, electrical transport, magnetic and optical properties, occurring due to the strong electron correlation effect in the systems. Further, TMO's possess some interesting phenomenon such as high Te superconductivity in cuprite system, metal insulator transition (MIT), colossal magneto resistance (CMR) and charge ordering in manganites [26].

In particular, the existence of metal-insulator transition phenomenon in La- based manganites was established in early 1950s [9,12] and was extensively studied thereafter. These types of perovskites present a very interesting group of materials because of extremely rich variety of their electrical properties from a large gap insulator to metal and magnetic properties such as nonmagnetic to magnetism, anti-ferromagnetism to ferromagnetism. Examples of these perovskites are LaFeO3, LaCoO3, LaCrO3, LaNiO3, LaMnO3 and certain doped manganites. The magnetic and electrical transport properties of these samples are determined by several factors such as the percentage of the divalent ions, the ionic radii of the metal ions, and the method used in preparation of samples[7,10].

Basically the name provskite refers to a relatively rare mineral called as calcium titanium oxide(CaTiO3)occurring in orthorhombic crystal symmetry and it is found in contact metamorphic rocks and associated mafic intrusivesneophelinesyenites and rare carbonates. The basic chemical formula follows the pattern ABO3in which A and B are cations of different size e.g. LaMnO3, more specifically, A is a rare earth element and B is transition metal element.

ISSN: 2277-9655
Impact Factor: 4.116

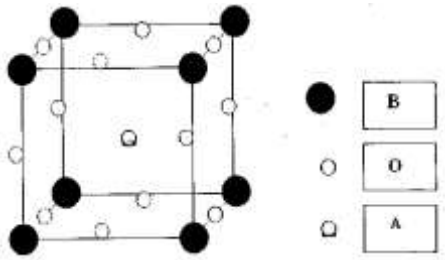

Figure 1. General perovskite structure(BCC)

The general crystal structure can be thought of as a body centered cubic (BCC) lattice with 'A' ion of valency +2 at the center surrounded by eight 'B' ion of velency +4 each at the corner at 12 'O' ions each occupies the edge.

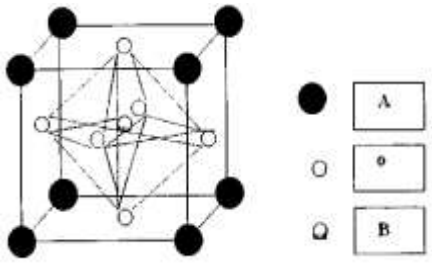

Figure 2. General perovskite structure(FCC)

The structure can be thought of as face centered cube (FCC) lattice with ion 'B' at the center surrounded by six 'O' ions, each at a face center and eight 'A' ions, each at the center[5].

For perovskite itself CaTiO3cubic symmetry is found at all temperatures but for compounds such as BaTiO3, PbTiO3, KNbO3there is slight adjustment to a tetragonal from of cooling below the ferroelectric transition temperature. The stability of a perovskite structure depends upon tolerance factor defined Goldschmidt tolerance factor and is formulated as:

$$t = (R_A + R_0) / [\sqrt{2R_B} + R_0$$

Where RA, RBand RO are ionic radii of A, B cation and oxygen respectively. However, for an ideal perovskite t=1 and for t<1, the cubic structure which leads to deviation in Mn-O-Mn bond angle from 180 degree (a case for ideal perovskite) the deviation of Mn-O-Mn bond angle from 180 degree leads to distortion in MnO6octahendra, for instance LaMnO3 is an orthorhombic perovskite structure and is an insulator[17].
Generally, the electrical and magnetic properties of these perovskites depend on the choice of elements A, B and doping element either at A or B site [2]. Moreover, perovskite structure has the curious property that the central atom does not touch its coordination neighbors in violation of Pauling's rules. This gives the structure, the property of piezoelectricity and sometime Ferro electricity. Oxides such as BaTiO3, LaNiO3, LaMnO3, LaFeO3etc, are known as representative compounds. These materials offer wide variety of phase transition like ferroelectric toantiferroelectric or purely structural transition. Most of the transition encountered in the perovskite crystal involves only a small change in the atomic position parameters, changes that leave the essential topology of thee structure unaltered. These change are often hard to detect directly and are detected indirectly by the changes or discontinuities in physical properties that are linked to the changes of atomic position parameter [1,22].

NATURE AND BEHAVIOR OF PEROVSKITE MATERIALS

Recently, a promising class of magnetic material with composition R1-xAxMnO3(R=La, Nd,Gd,Y; A= Ca, Sr, Ba, Pb) has been identified. Most of the studies in these materials were done by replacing La by divalent elements. The basic structural, magnetic and transport properties of oxides La1-xAxMnO3(A= Ca, Sr, Ba, Pb) were widely studied. Recently, tetravalent cation doped manganites, including Ce, Sn, Te, Zr have gradually attracted much attention since such tetravalent cation doping may drive the valence state of Mn3+ in the parent compound into the mixed state of Mn3+and Mn2+. This is known as electron doping and such compounds are known as the electron doped manganites[14,15].

Generally, all the manganese ions in LaMnO3family compound are considered as in a mixed valence state of Mn3+-Mn4+ ion has electron configuration of t32g e1g. The low energy t32gtriplet state contribute a local spin of S= 3/2, while eg electron is either itinerant electrons hop between Mn3+ and Mn4+, and the hoping probability depends on Mn-O-Mn bond angle and relative orientation of the local spin. This kind of physical picture can be qualitatively depicted in the CMR mangestoresistance behavior[28].

Later on, some reports on Ce doped LaMnO3appeared in the La1-xCaxMnO3system, where Ce is a tetra-valent ion, was electron–doped system. The reports suggested that the CMR behavior probably occurred in a system of mixed valence state Mn2+- Mn3+. Therefore, it is of great interest to investigate whether the CMR effect exists in the compounds in which La3+ is partially replaced by tetra–valence element [29].

THEORY

The basis for the theoretical understanding of Mn oxides is usually the concept of the double exchange (DE) that consider the exchange of electron between neighboring Mn3+ and Mn4+ sites with strong on – site Hunds coupling. Perturbative calculation carried out by Millis et al. showed that DE alone could not explain the experimental data of Mn oxides and suggested that a strong Jahn –Teller distortion should be responsible for the transport properties.[1, 8] Later on it was suggested that the localization effect [4, 6] in the double exchange model based upon non perturbative treatment might be able to account for the novel properties of manganites.The theory of variable range hoping has been quite successful in describing the conductivity in insulating sample, due to Mott[5,27] who formulated an approach using ideas from percolation theory. A good discussion of Mott's original approach also appears in [26].

In general Mott's VRH model describes the low temperature behavior of the resistivity in strongly disordered system where states are localized. Consider two states located a distance R apart. The state on the left hand side is at energy E1 and that on the right hand side is at energy E2. Suppose W = E2 - E1>0. An electron can hop from left to right by the absorption of phonon with energy ω. The hopping rate is given by:

$$\frac{1}{\tau_R} = \omega_o e^{-2r/a} f_1(1-f_2)n(W) \qquad \dots\dots\dots\dots\dots\dots\dots\dots\dots\dots (1)$$

Whereω_o, is the attempt frequency which is given by typical phonon frequency. A is the localization length, n(W) is the Bose factor and $f_1 = \frac{1}{\frac{E_i-\mu_i}{e\ kt}+1}$ is the Fermi factor for states i=1 and 2 with chemical potential μ1and μ2. The hopping rate for right to left by the emission of phonons is:

$$\frac{1}{\tau_L} = \omega_o e^{-2r/a} f_2(1-f_1)\{n(W)+1\} \qquad \dots\dots\dots\dots\dots\dots\dots\dots (2)$$

The current is:

$$I = eR\left[\frac{1}{\tau_R} - \frac{1}{\tau_L}\right] \dots\dots\dots\dots\dots\dots\dots\dots\dots\dots\dots\dots\dots\dots\dots\dots\dots (3)$$

Current in terms of chemical potential:

$$I = \frac{eR\omega_o}{kT} e^{-W/kT} e^{-2r/a}(\mu_1 - \mu_2) \dots\dots\dots\dots\dots\dots\dots\dots\dots\dots\dots (4)$$

With the help of above we can found the expression for the conductance as

$$G = \frac{e^2 R\omega_o}{kT} e^{-W/kT} e^{-2r/a} \dots\dots\dots\dots\dots\dots\dots\dots\dots\dots\dots (5)$$

The key insight to Mott is that G should be determined by optimizing the competition between the overlap terme$^{-2r/a}$, which favors short hops and the energy activatione$^{-W/kT}$, which favours long hops. With longer hops; one has a better chance of reducing the activation energy W. We estimate W by the typical energy level spacing in volume with radius R.

$$W = \frac{3}{4\pi r^3 N(E_F)} \dots\dots\dots\dots\dots\dots\dots\dots\dots\dots\dots\dots\dots\dots (6)$$

Where $N(E_F)$ is the density of states at Fermi energy. By substituting the value of W from E.q 6in 5 we find:

$$\bar{R}^4 = \frac{9a}{4\pi N(E_F)kT} \dots\dots\dots\dots\dots\dots\dots\dots\dots\dots\dots\dots\dots\dots (7)$$

And the conductance

$$G \approx \exp(-T/T_0)^{\frac{1}{4}} \dots\dots\dots\dots\dots\dots\dots\dots\dots\dots\dots\dots\dots\dots (8)$$

Where T_0 is related to the average energy spacing in a volume a3 as:

$$kT_o = \frac{1}{N(E_F)a^3} \dots\dots\dots\dots\dots\dots\dots\dots\dots\dots\dots\dots\dots\dots (9)$$

Eq. 8 is the famous Motts variable range hopping (VRH) law [20]

The electrons in a solid interact both with one another and with the lattice vibrations. Interaction with phonons also has an important effect, particularly in transition metal oxides, i.e. they interact with the electrons or holes in a narrow band semiconductor or semimetal, forming polarons.

The behavior of polarons is of great importance in particular to transition metal oxides. In the polar material a polaron is the region round an electron in the conduction band in which the material is polarized by the electron, as first proposed by landau (1993). The field in vivinity of the electron, with which it interacts,has a potential energy function:

$$V(r) = -\frac{e^2}{k_p r}, r > r_p \dots\dots\dots\dots\dots\dots\dots\dots (10)$$

$$= -\frac{e^2}{k_p r_p}, r > r_p$$

Where $1/k_p = 1/k_\infty - 1/k$ and k_∞, k are the high frequency and static dielectric constants in principle.The radius of polaron,r_p, is determined by minimizing the polaron's energy. Which is made up of the energy of the electron in a polaron well

$$= -\frac{e^2}{k_p r_p} + \frac{h^2\pi^2}{2m^* r_p^2} \dots\dots\dots\dots\dots\dots\dots\dots\dots\dots\dots\dots (11)$$

Where m^* is the effective mass.The energy required to polarize the medium

$$= \frac{1}{2} e^2/k_p r_p$$

If r_p is larger than the lattice parameter, the polaron is called a large or Fröhlichpolaron and its properties depend on the dimensionless coupling constant α, defined by

$$\alpha^2 = \left(\frac{e^2}{k_p}\right)\sqrt{\left(\frac{m^*}{3h^3\omega_0}\right)} \dots\dots\dots\dots\dots\dots\dots\dots\dots\dots (12)$$

The polaron is called small polaron when r_p has its limiting size,

$$r_p = \frac{1}{2}\left(\frac{\pi}{6N}\right)^{1/3} \dots\dots\dots\dots\dots\dots\dots\dots\dots\dots\dots\dots (13)$$

Where N is number of sites per unit volume.The energy of small polaron$-W_p$ is given by

$$W_p = \frac{1}{2}\left(\frac{e^2}{k_p r_p}\right) \dots\dots\dots\dots\dots\dots\dots\dots\dots\dots\dots\dots (14)$$

The small polaron has the following properties:

At high temperature [$T>\frac{1}{2}\theta_D$] it moves by 'hoping'.The frequency with which it 'hops' from one site to another is given by the relation.

ISSN: 2277-9655
Impact Factor: 4.116

$$\omega = \exp\left(\frac{-W_H}{kT}\right) \ldots\ldots\ldots\ldots\ldots\ldots\ldots\ldots\ldots\ldots\ldots\ldots\ldots\ldots\ldots\ldots\ldots (15)$$

Where

$$W_H = \frac{e^2}{4k_p}\left(\frac{1}{r_p} - \frac{1}{R}\right) \ldots\ldots\ldots\ldots\ldots\ldots\ldots\ldots\ldots\ldots\ldots\ldots\ldots\ldots\ldots\ldots (16)$$

And R is the distance from one site to another, W_H is the energy of intermediate state, where thermal fluctuation have decreased the depth of the potential well and produced an empty potential well on neighborhood site so that an electron can resonate between the two wells. Equation 16 is valid only in so called adiabatic approximation, which means that an electron can go backwards and forward several times during the period when the two wells have the same depth. At low temperatures,$T < \frac{1}{2}\theta_D$, the electron moves from site to site without the aid of thermal activation. At zero point energy $\frac{1}{2}\hbar\omega$ due to thermal vibration, the hoping frequency becomes:

$$\omega = \exp\left(\frac{-W_H}{\frac{1}{2}\hbar\omega}\right) \ldots\ldots\ldots\ldots\ldots\ldots\ldots\ldots\ldots\ldots\ldots\ldots\ldots\ldots\ldots\ldots\ldots (17)$$

It can be seen from elementary considerations, the distortion of surrounding medium which leads to intermediate state with energy W_H can be described by simple harmonic motion, with a parameter ξ for the displacement, a potential energy $\frac{1}{2}p\xi^2$ and a wave function of the form $\psi = \text{const}\exp(-\alpha\xi^2)$. The probability $|\psi|^2$ for a configuration with potential energyW_H is thus:

$$\exp\left(\frac{-2\alpha W_H}{\frac{1}{2}p}\right) \ldots\ldots\ldots\ldots\ldots\ldots\ldots\ldots\ldots\ldots\ldots\ldots\ldots\ldots\ldots\ldots\ldots (18)$$

And putting in the constant it is easy to see that:

$$\frac{4\alpha}{p} = \left(\frac{1}{\frac{1}{2}\hbar\omega}\right) \ldots\ldots\ldots\ldots\ldots\ldots\ldots\ldots\ldots\ldots\ldots\ldots\ldots\ldots\ldots\ldots\ldots (19)$$

Energy level scheme of LaMnO3 and Jahn Teller distortion and effect

In LaMnO3, Mn exists in +3 states (3d4). There are four electrons in d-orbital. Due to crystal field splitting 3 electrons go to 't2g' level and the remaining one electron goes to 'eg' level. We know that Jahn-Teller distortion will be effective only when 'eg'orbitals are asymmetrically filled here 'eg' orbital contain only one electron i.e. asymmetrically filled and it is, thus, Jahn-Teller active. Due to this Jahn-Tellerdistortion the MnO6octahedra distort in such a way that there are long and short Mn-O bonds [15,22]. This occurs below a characteristic temperature (Tjt). Due to this JT distoration the oxygen ion is displaced by ≥ 0.1,Åsplitting of the 'eg'level occurs and opens a gap at Fermi level [28,29].

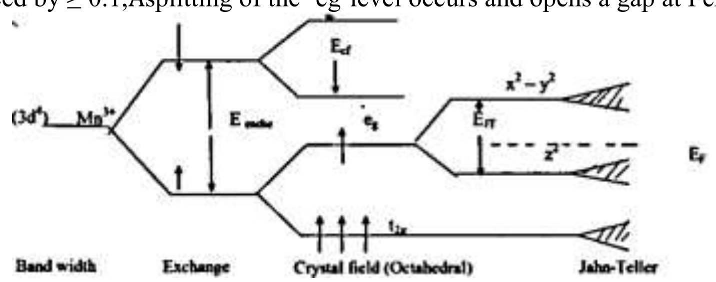

Figure 3. Energy level of scheme for LaMnO3

In Figure 3, we have shown a schematic of the band diagram of LaMno3 that elucidate how JT distortion splits the conduction band makes the material insulating.

Effect of doping in Manganites and Zener Double Exchange Interaction

Generally manganites Mn exists in three states Mn+2, Mn+3 and Mn+4 in orthorhombicallydistorted octahedral with 3d5, 3d4 and 3d3 configuration respectively. The doping of a divalent cationat the rare earth site converts a proportionate amount of Mn+3ion into Mn+4 i.e. Mn+3-Mn+4 system have been obtained. We have already known that in Mn+3 system there is single electron in (^5e_g)and is J-T active. One the other hand Mn+4ion has no 'eg'electron as all 3 electrons go to the 't2g'level. Therefore there is rise to a vacancy (hole) in theMn+3-Mn+4 system. Due to strong correlation effect the't2g' electrons are localized where the 'eg' electrons can hop depending on the relative configuration of the local spins. The hopping of 'eg' electron can be demonstrated by Double Exchange Interaction [14, 15, 22]

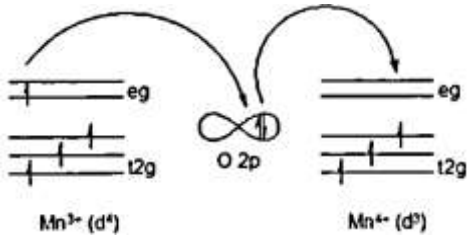

Figure 4. Double Exchange Model

Here an electron from Mn+3 jumps to Mn+4 via the oxygen ion. According to the Double Exchange Interaction the electron movement from one species to another will be facilitated more easily if the electrons do not have to change spin direction in order to conform with Hund's rules when on the accepting species. The jump of electron from one species to another species leads to increase of conductivity and it also leads to ferromagnetic alignment of neighboring ions.

On the other hand if tetravalent ion (Zr+4) ion is doped a proportionate amount ofMn+3 ion is likely to be converted into divalent state Mn+2 that is Mn+3-Mn+4 system is obtained. In this case there is one electron in the 'eg' band corresponding to Mn+3. But for Mn+2(3d5) there is no first order crystal field splitting as for d5 term not crystal field stabilization is zero. Thus, in such a system the interaction between the 'eg' electron and the 'd' electron should be large that would cause a change in CMR effect[2].

Experimental Methods:

In order to determine the structure of different crystals a highly significant law in solid state physics is Bragg's Law. Crystals are composed of various intersecting planes each of which itself contains a number of atoms. Since the interatomic separations in crystals are of the same order of magnitude as the wavelength of x–xray crystals act as diffraction gratings and produce diffraction on being irradiated by x–ray.

If each plane were perfectly reflecting, only the first plane of a parallel set would see the radiation and any wavelength would be reflected, but each plane reflects 10-3 to 10-5 of the incident radiation, so that 103 to 105 planes may contribute to the formation of Bragg's reflected beam in a perfect crystal.

The x–ray gets diffracted from the crystal planes when the Bragg's condition is satisfied i.e $2d\sin\theta=n\lambda$. Where d is the interplaner spacing, n is the order of diffraction, λ is the wavelength of x–ray and θ is the glancing angle.

By measuring 2θ one can determine the spacing d between the planes in the crystal. The diffraction pattern gives us information about the average particle/ grain size, lattice parameters, crystal structure of the sample etc.

ISSN: 2277-9655
Impact Factor: 4.116

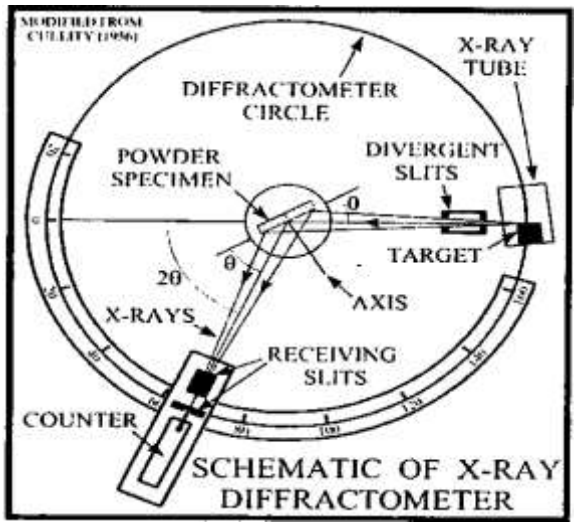

Figure 5. The schematic of x-ray diffractometer

Figure 3, shows that the XRD patterns are recorded with diffractometer. X–ray diffraction (XRD) is a powerful tool for studying both x–ray spectra and the arrangement of atoms in crystals. To study the spectra, a particular set of crystal planes having a known spacing'd' is chosen. These planes effectively reflect different wavelengths at different angles. A detector that can discriminate one angle from another can then be used to determine the wavelength of radiation reaching it. The crystal itself can be studied with a monochromatic x–ray beam, to determine not only the spacing of various crystal planes but also the structure of the unit cell. The recorded diffraction pattern gives the intensity versus 2θ plot.

Most common way of measuring the resistivity of a semiconducting material is the four-point collinear probe method.

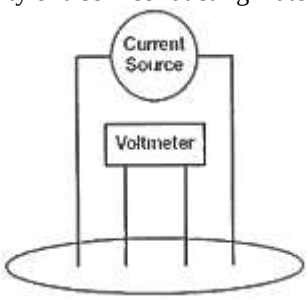

Figure 6. Four pint collinear probe resistivity configuration

Figure 4, shows the technique that involves bringing four equally spaced probes in contact with a material of unknown resistance. The probe array is placed in the center of the material. The two outer probes are used for sourcing current and the two inner probes are used for measuring the resulting voltage drop across the surface of the sample.
The volume resistivity is calculated as follows:

$$\rho = \frac{\pi}{\ln 2} \times \frac{V}{I} \times t \times k$$

Where, ρ represent volume resistivity, V represent the measured voltage, I represent the source current,t represent the sample thickness and k represent a correction factor based on the ratio of the probe of wafer diameter and on the ratio of wafer thickness to probe separation.
The resistivity of the semiconductor is often determined using this technique. Four probes eliminate measurement errors due to the probe resistance, the spreading resistance under each probe and the contact resistance between each metal probe and semiconductor material. Because a high impedance voltmeter craws little current, the voltage drops across the resistance, spreading resistance and contact resistance are very small.

ISSN: 2277-9655
Impact Factor: 4.116

RESULTS AND DISCUSSION

The structural parameters were refined by the standard rietveldtechnique [32]. The calculated parameters of prepared sample for x=0.10, 0.15 are shown in Figure7, and tabulated in Table 1.

Table 1. Lattice parameters and unit cell volume of La1-xTexMno(x=0.10 and 0.15) at room temperature.

Composition	a (Å)	b (Å)	c (Å)	Type of the unit cell	Volume (mn)3
La0.90Te0.10MnO3	5.526	5.526	13.350	Hexagonal	353.03
La0.85Te0.15MnO3	5.524	5.524	13.351	Hexagonal	352.80

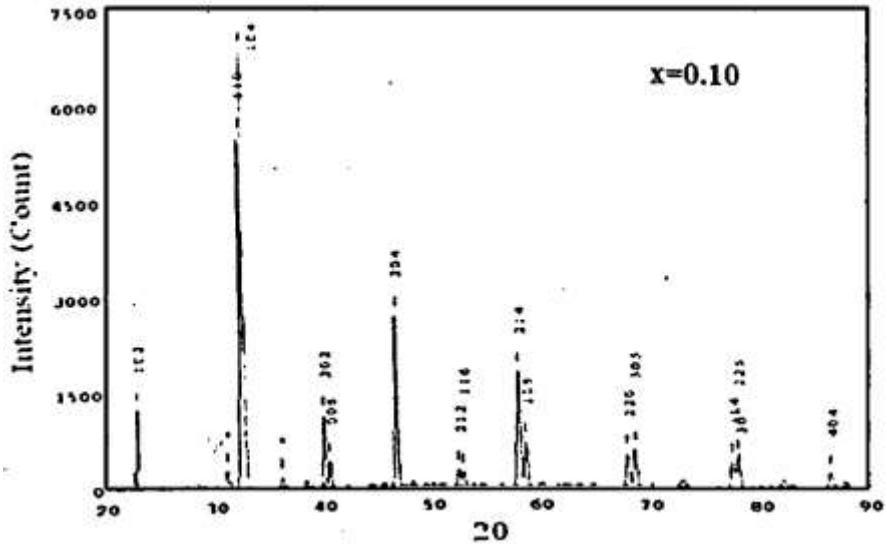

Figure 7. Power XRD pattern of $La_{1-x}Te_xMno(x=0.10)$

Figure 7, showsat the room temperature x–ray diffraction (XRD) patternsof La1-xTexMno(x=0.10) confirmed single phase nature of the sample with a few secondary phase peaks. This is consistent with many earlier reports on electron doped manganites [13,19].The lattice parameters (a, b, c) with the values (5,526,5.526,13.350)Å respectively, rhombohedral (Hexagonal) crystal structure with space group R3c, while the crystalline size of the sample is 34.60nm and the volume was 353.03nm3.

ISSN: 2277-9655
Impact Factor: 4.116

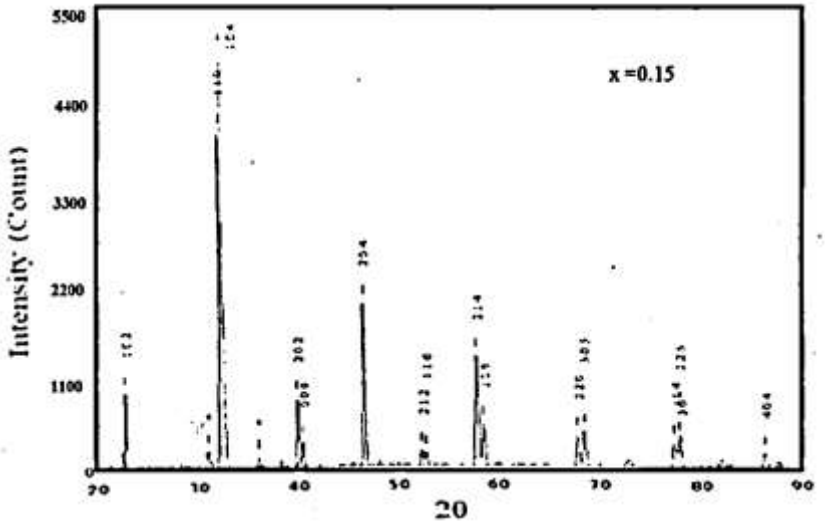

Figure 8. Power XRD pattern of $La_{1-x}Te_xMno(x=0.15)$

Figure 8,showsat the room temperature x–ray diffraction (XRD) patternsof La1-xTexMno(x=0.10) confirmed single phase nature of the sample with a few secondary phase peaks.This is consistent with many earlier reports on electron doped manganites [13,19]. The lattice parameters (a, b, c) with the values (5,524, 5.524, 13.351)Å respectively, rhombohedral (Hexagonal) crystal structure with space group R3c, while the crystalline size of the sample is 37.76nm and the volume was 352.80nm3

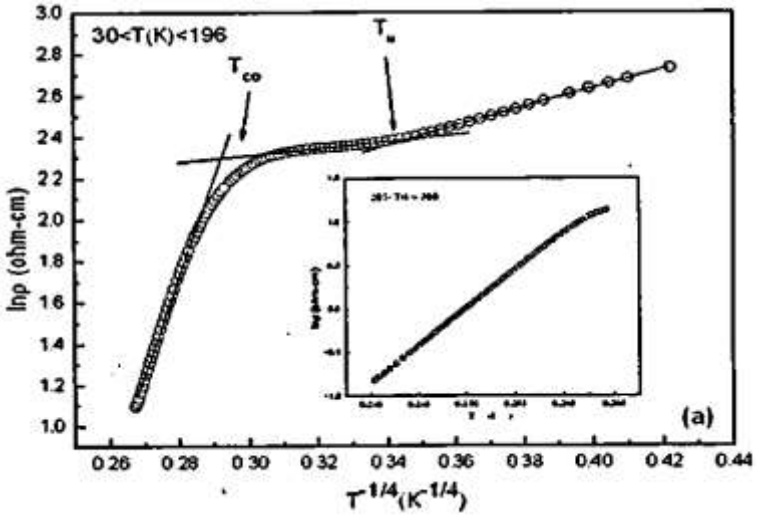

Figure 9. Shows that in ρ(T) as a function of $1/T^{1/4}$ for $La_{0.90}Te_{0.10}MnO_3$.

Figure9,shows that in ρ(T) as a function of 1/T1/4for La0.90Te0.10MnO3. The resistivity ρ(T) data showed to be fitted with purely activated conduction model. ρ(T) =ρ0(T)exp(Ea/kBT), three dimensional Mott's variable range hopping (VRH) model[20,21], ρ(T) =ρ0(T) exp(To/T)1/γ, with γ =4, predicting the charge transport by tunneling of electrons or holes[36], γ=4 has been considered as an indicative for isotropic charge transport.

ISSN: 2277-9655
Impact Factor: 4.116

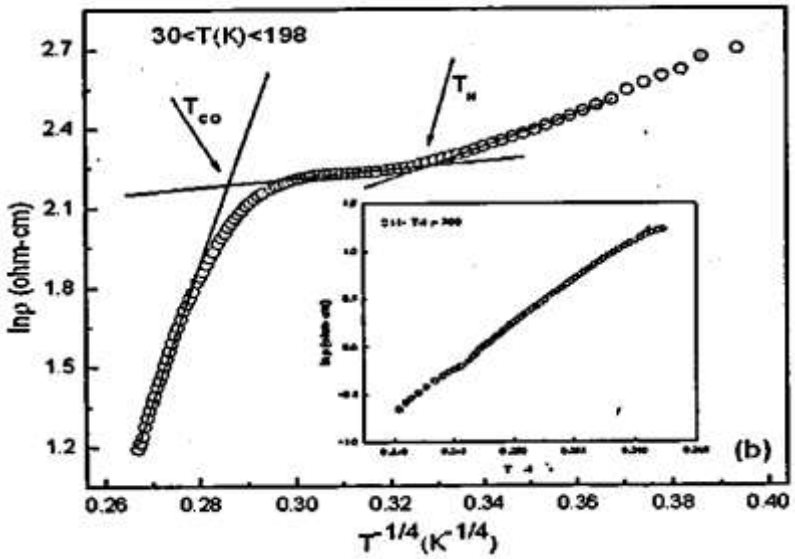

Figure 10. Shows that in ρ(T) as a function of $1/T^{1/4}$ for $La_{0.85}Te_{0.15}MnO_3$.

Figure10, shows that in ρ(T) as a function of 1/T1/4for La0.85Te0.15MnO3, the resistivity ρ(T) data showed to be fitted with purely activated conduction model. ρ(T) =ρ0(T) exp(Ea/kBT), three dimensional Mott's variable range hopping (VRH) model, ρ(T) =ρ0(T) exp(To/T)1/γ, with γ= 4, predicting the charge transport by tunneling of electrons or holes[36], γ=4 has been considered as an indicative for isotropic charge transport.

Table 2. Values of characteristic temperature to, density of states at the Fermi energies N(EF) and chi-square (x2) determined from fitting of resistivity–temperature data for La1-xTexMnO3(x=0.10 and 0.15).

Concentration	Temperature ranges	to(K)	N(EF)(eV-1.cm-3)	x2
0.10	Above ρ(T)	560x105	2.09x1026	0.9996
	T>TCO	485x104	2.42x1027	0.9959
	TN<T<TCO	7.86	1.49x1033	0.9800
	T<TN	437.71	2.68x1031	0.9996
0.15	Above ρ(T)	660x105	1.78x1026	0.9985
	T>TCO	677x104	1.74x1027	0.9952
	TN<T<TCO	7.7	1.52x1033	0.9240
	T<TN	1923.48	6.11x1030	0.9965

ISSN: 2277-9655
Impact Factor: 4.116

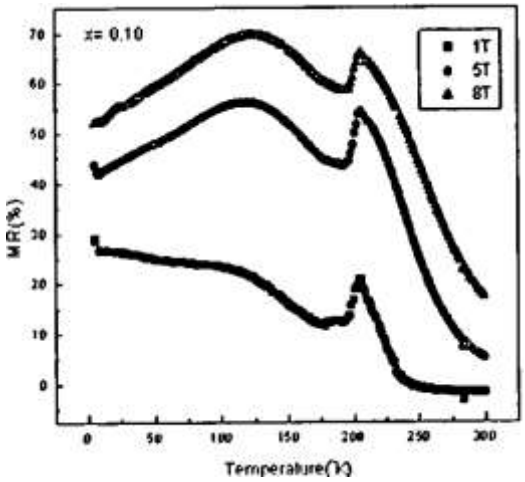

Figure 11. Temperature dependence of magneto-resistance (MR) measured in the presence of magnetic field of 1T, 5T and 8T for $La_{1-x}Te_xMnO_3$ (x=0.10).

Figure 11, shows that at fitting of resistivity temperature data for La1-xTexMno(x=0.10) various temperature range occurs. The values of characteristic temperature To can be given as the following above Tp we got 560x105K, density of state at the Fermi energies[28] was2.09 x1026 and the chi-square x2 was 0.9996. Similarly when T>TCO, TN<T<TCO and T<TN as shown in Table 2.In the presence of the magnetic fields[8T,5T,1T], sharp and broad peaks can be attributed to the co–existence of the antiferromagnetic and ferromagnetic clusters, the phase co-existence features is explained in the frame work of electronic phase separation scenario, predicated for the manganites[3]. This behavior is attributed to the structural inhomogeneity's characteristic of ceramic sample that governs the electric and magnetic properties.

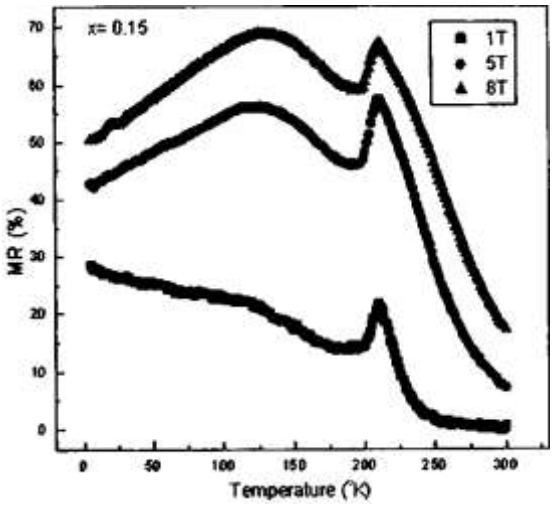

Figure 12. Temperature dependence of magneto-resistance (MR) measured in the presence of magnetic field of 1T, 5T and 8T for $La_{1-x}Te_xMnO_3$ (x=0.15).

Figure12, shows that at fitting of resistivity temperature data for La1-xTexMno(x=0.15)various temperature range occurs. The values of characteristic temperature To can be given as the following above Tp we got 660x105K, density of state at the Fermi energies[28] was 1.78 x1026and the chi-square x2 was 0.9985. Similarly when T>TCO, TN<T<TCO and T<TN as shown in Table 2.In the presence of the magnetic fields [8T,5T,1T], sharp and broad peaks

ISSN: 2277-9655
Impact Factor: 4.116

can be attributed to the co – existence of the antiferromagnetic and ferromagnetic clusters, the phase co –existence features is explained in the frame work of electronic phase separation scenario, predicated for the manganites[3]. This behavior is attributed to the structural inhomogeneity's characteristic of ceramic sample that governs the electric and magnetic properties.

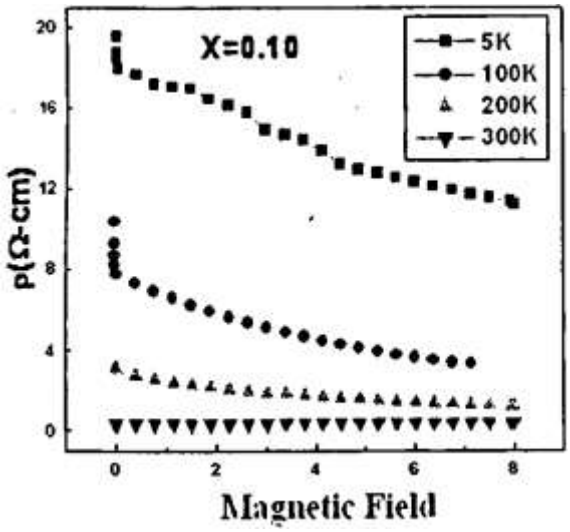

Figure 13. Magnetic field verses resistivity ρ(Ω–cm) at different temperature (300K,200K,100Kand 5K) for $La_{1-x}Te_xMnO_3$ (x=0.10).

Figure 13, shows that on decreasing the temperature for La1-xTexMnO3 (x=0.10), the compound first undergoes insulating to metallic phase at transition temperatures Tp = 203 and 209o respectively, then resuming the semiconducting behavior. A wide band centered between 70o to 140oK is observed as a consequence of charge ordering transition in the sample. at high temperature 300K the magnetic field verses resistivity ρ(Ω–cm) will remain constant, while the temperature at 200Kthe magnetic field verses resistivity ρ(Ω–cm)will slightly decrease, moreover, decreasing in temperature leads to increasing in magnetic field and increasing in verses resistivity ρ(Ω–cm) till it reaches 20.

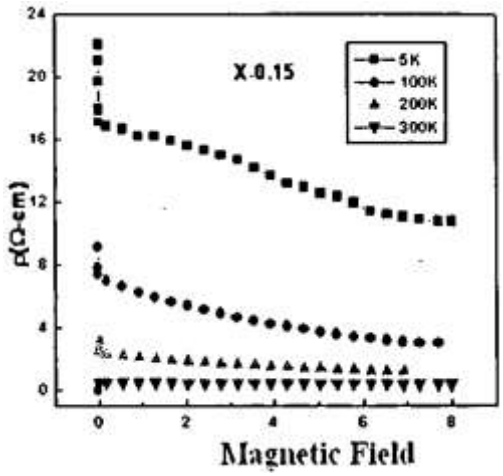

Figure 14. Magnetic field verses resistivity ρ(Ω–cm) at different temperature (300K,200K,100Kand 5K) for $La_{1-x}Te_xMnO_3$ (x=0.15).

Figure 14, shows that on decreasing the temperature for La1-xTexMnO3 (x=0.15), the compound first undergoes insulating to metallic phase at transition temperatures Tp = 203 and 209o respectively, then resuming the semiconducting behavior. A wide band centered between 70o to 140oK is observed as a consequence of charge ordering transition in the sample. At high temperature 300K the magnetic field verses resistivity ρ(Ω–cm) will remain constant, while the temperature at 200Kthe magnetic field verses resistivity ρ(Ω–cm) will slightly decrease, moreover, decreasing in temperature leads to increasing in magnetic field and increasing in verses resistivity ρ(Ω–cm) till it reaches more than 20. The strong increment of the resistivity with decreasing temperature can be described by the Mott's variable (VRH) model[35]. It is assume that the charge carries move along a path described by the optimal pair hopping from one localized state to another.

CONCLUSION

We have systemically investigated the structural and electronic transport properties for La1-xTexMnO3 (x=0.10 and 0.15) and our finding may be summarized as follows:

We have studied the crystal structure using x –ray diffraction technique with the help of POWDER-X software we have determined the lattice parameters, unit cell volume, crystallite size and crystal symmetry for different compositions. We have found that, the unit cell volume of the sample decreases with the increase in Te concentration, the crystallite size increase with the increase in Te concentration, it has rhombohedral (hexagonal crystal symmetry.

The temperature dependent resistivity ρ(T) plots for La1-xTexMnO3 (x=0.10 and 0.15) has been studied, on decreasing the temperature these compounds first undergo insulating to metallic phase transition at transition temperatures Tp=203 and 209oK respectively, then resuming the semiconducting behavior, a wide band centered between 70 to 140oK is observed as a consequence of charge ordering transition in both the samples.

The samples are found to be in single phase. The charge ordering transition temperature of La1-xTexMnO3 is enhanced with in Te concentration (Tco=125o to 135oK), while the magneto resistance is suppressed slightly. Below and above the CO transition temperature, the transport behavior is dominated by Mott's variable range hopping (VRH) mechanism.

The magneto resistance as a function of temperature is also studied in the presence of magnetic of the magnetic fields, sharp and broad peaks can be attributed to the co–existence of the antiferromagnetic and ferromagnetic clusters, contributing the spatially metallic and insulating areas in the studied temperature.

REFERENCES

[1] A. J. Millis, B. I. Shaiman and R. Mueller; Phys. Rev. Lett. 77, 175(1996).
[2] A. J. Millis, P. B. Littlewood and B. I. Shaiman; Phys. Rev. Lett. 74,5144(1995).
[3] A. Moreo, S. Yukoni, and E. Dagoto, Science 283 (1999) 2034.
[4] A. Urushibara, Y. Moritomo, T. Arima, A. Asamitsu, G. Kido, Y. Tokure. Phys. Rev. B51 (1995)14103.
[5] B. I. Shklovskii and A. I. Efors, Electronic Properties of Doped Semiconductors (springer – verlag, Berlin, 1984).
[6] C. M. Varma; Phys. Rev. B54, 7328 (1996).
[7] D.D. Sharma, N. Shanthi, S. R. Barman, N. Hamda, H. Sawadana and K. Terakura, Phys. Rev .Lett. 75, 3336 (1995).
[8] E. Muller – Hartmann and E. Doggoto; Phys. Rev. B54, E 6819 (1996).
[9] G.H. Jonker and J.H. van Santen; Physica 16, 377 (1950).
[10] G. Pari, S.M. Jaya, G. Subramniam and R. Asokamni, Phys. Rev. B51, 16575 (1995).
[11] H. Y. Hwang, S.-W.Cheong, P.G. Radaelli, M.Marezio, and B. Batlogg, Phys. Rev. Lett. 75,3336(1995).
[12] J.H. van Santen and G.H. Jonker; 16, 599 (1950).
[13] J. L. Cohn, M. Peterca and J. J. Neumeier, J. Appl. Phys. Rev. B 72(2005) 034102.
[14] J. M. D.Coey, M. Viret, S.von Molnar, Adv. Phys. 48 (1999) 167.
[15] K. Chahara, T. Ohno, M.Kasai and Y. Kozono, Appl. Phys. Lett. 63(1993)1990.
[16] L.X. He, J.B. Neaton, M.H. Ceon, D. Vanderbilt and C.C. Homes, Appl. Phys. Rev. B65 (2002) 214112.
[17] M. A. Kastner et al. Phys. Rev. B 37 (1988) 111; C. Uher and A. B. Kaiser, Phys. Rev. B 37 (1988) 127.
[18] M. H. Ceon, J. B. Neaton, L. X.He, and D. Vanderbilt J. Appl. Phys. 94(2003) 3299.L. X.He, J. B. Neaton, M. H. Cohen, D. Vanderbilt, and C.C. Homes, phys. Rev. B 65 (2002) 214112.
[19] N. Bskup, A. de Anders, J.L. Martinez, et al., Appl. Phys. Rev. B 72(2005) 024115.

[20] N.F. Mott, J. Non – cryst. Sol. 1, 1(1968).
[21] N.F.Mott, Philos. Mag. 19 (1969) 835; Rev. mod. Phys. 50(1978) 203.; N.F. Mott and E.A.Davies. Electronic processes in non crystalline materials (Oxford Univ. press Oxford(1971).
[22] P. G. Radaelli. D. E. Cox. L. Capogna, S.W.Cheong, M. Marezio, . Phys. Rev. B59 (1999) 4440.
[23] R.Von. Helmolt, J. Wecker, B. Holzapfel, L. Schulta and K. Samwer, Phys . Rev. lett. 71(1993) 2331.
[24] S. Jn, T. H. Tiefel, M. M. Cormack, R. A. Fastnacht, R. Ramesh, L. H. Chen Science, 264 (1994) 413.
[25] S. Yunoki, T. Hotta,Phys . Rev. lett. 84(2000) 3714.
[26] Text Book on Metal Insulator Transition by N.F. Mott, Taylor and France Ltd 1974, pp. 55.
[27] Vinayambegaokar, B. I. Halperin and J. S. Langer; ; Phys. Rev. B54, 2612 (1971).
[28] Y. Tokura, N. Nagaosa, Science 288 (2000) 4.
[29] Y. Tokura, Y.Tomioka, H. Kuwahara, A. Asamitsu, Y. Moritomo, M. Kasai, J. Appl. Phys. 79 (1996) 5288.